Brief Definitive Report

The Tumor Suppressor CYLD Interacts with TRIP and Regulates Negatively Nuclear Factor κB Activation by Tumor Necrosis Factor

Alexandre Regamey,[1] Daniel Hohl,[1] Jia Wei Liu,[1] Thierry Roger,[2] Priit Kogerman,[3,4] Rune Toftgård,[3] and Marcel Huber[1]

[1]*Department of Dermatology, and* [2]*Division of Infectious Diseases, Department of Internal Medicine, CHUV, Lausanne 1011, Switzerland*

[3]*Department of Bioscience, NOVUM, Karolinska Institutet, Huddinge 141 57, Sweden*

[4]*Laboratory of Molecular Genetics, National Institute of Chemical Physics and Biophysics, and Department of Gene Technology, Tallinn Technical University, Tallinn 12618, Estonia*

Abstract

Cylindromas are benign adnexal skin tumors caused by germline mutations in the CYLD gene. In most cases the second wild-type allele is lost in tumor tissue, suggesting that CYLD functions as tumor suppressor. CYLD is a protein of 956 amino acids harboring a functional deubiquitinating domain at the COOH-terminal end. To shed more light on the function of CYLD, we have performed a yeast two hybrid screen using an HaCaT cDNA library that identified the RING finger protein TRIP (TRAF-interacting protein) as interactor with full-length CYLD. Mapping of the interacting domains revealed that the central domain of CYLD binds to the COOH-terminal end of TRIP. Far Western analysis and coimmunoprecipitations in mammalian cells confirmed that full-length CYLD binds to the COOH-terminal domain of TRIP. Because TRIP is an inhibitor of nuclear factor (NF)-κB activation by tumor necrosis factor (TNF), the effect of CYLD on NF-κB activation was investigated in HeLa cells. The results established that CYLD down-regulates NF-κB activation by TNF-α. The inhibition by CYLD depends on the presence of the central domain interacting with TRIP and its deubiquitinating activity. These findings indicate that cylindromas arise through constitutive NF-κB activation leading to hyperproliferation and tumor growth.

Key words: cylindroma • skin tumor • epidermis • keratinocyte • inhibition

Introduction

Cylindromas are benign adnexal tumors that most likely arise from the eccrine or apocrine cells of the skin (1, 2). They emerge in the second or third decade of life in hairy areas of the body, but never on the palms and soles where apocrine glands are absent (3). They accumulate in number and grow slowly throughout life, sometimes forming a confluent disfiguring mass on the scalp (turban tumor syndrome). The familial form of cylindromatosis is inherited as an autosomal dominant predisposition to multiple adnexal skin tumors which has been mapped to chromosome 16q12-13 by genetic linkage analysis (4–8). Mutational analysis in genes localized to the candidate interval revealed mutations in a single gene, CYLD, in both the germline of 21 cylindromatosis families and sporadic cylindromatosis cases (9). Most of the mutations are premature stop codons leading to proteins truncated in the second half of the protein. Genetic data indicate that CYLD is a tumor suppressor gene (4, 7, 10). There are no indications that CYLD inactivation leads to chromosomal instability (9). Abrogation of CYLD alleles could promote neoplastic transformation by promoting cell proliferation and/or inhibition of apoptosis.

The CYLD gene is expressed ubiquitously, which seems to be difficult to reconcile with the localized body distribution of cylindromas. The protein encoded by the CYLD gene comprises 956 amino acids (aa; reference 9). Protein motif searches (9) of CYLD revealed three regions in the NH_2-terminal half exhibiting weak homology to a glycine-rich region found in some cytoskeleton-associated proteins (CAP-Gly domain; reference 11). The COOH-terminal

Address correspondence to Marcel Huber, Department of Dermatology, CHUV, Avenue Beaumont 29, BT-421, Lausanne 1011, Switzerland. Phone: 41-21-3140374; Fax: 41-21-3140378; email: Marcel.Huber@chuv.hospvd.ch

 J. Exp. Med. © The Rockefeller University Press • 0022-1007/2003/12/1959/6 $8.00
Volume 198, Number 12, December 15, 2003 1959–1964
http://www.jem.org/cgi/doi/10.1084/jem.20031187

part of CYLD displays partial homology to the active sites of ubiquitin-specific proteases (12, 13). This enzymatic activity of CYLD was confirmed by a chemistry-based approach (14), indicating that CYLD could deubiquitinate target proteins.

To elucidate the functional role of CYLD at the molecular and cellular level in adnexal tumor suppression, we sought to determine molecular partners of CYLD. This identified TRIP (TRAF-interacting protein) as a CYLD interactor, and reporter assays demonstrated an inhibitory role of CYLD in TNF-α–mediated nuclear factor (NF)-κB activation. This suggests that loss of CYLD leads to deregulation of NF-κB signaling giving rise to neoplasia in epidermal adnexal tissue.

Materials and Methods

Yeast Two Hybrid Screen. Full-length and partial cDNAs encoding CYLD and candidate proteins were cloned into the pGBKT7 or pGADT7 vectors (CLONTECH Laboratories, Inc.), respectively. Screening for interactors was performed in the AH109 yeast strain on high stringency plates (SD/-ade-his-leu-trp, 10 mM 3-amino-1,2,4-triazole, 20 μg/ml 5-bromo-4-chloro-3-indolyl-β-D-galactopyranoside). Activity of α-galactosidase in culture medium was measured with para-nitrophenol-α-galactopyranoside (Sigma-Aldrich). Candidate clones and constructs were analyzed by sequencing.

Mammalian Cell Expression. pCYLD1 and pCruzCYLD1 were constructed by insertion of full-length CYLD cDNA either in pMT2 (15) or pCruzHA vector (Santa Cruz Biotechnology, Inc.) to express proteins NH_2 terminally tagged with FLAG or HA, respectively. Premature stop codons were introduced by PCR. Complete TRIP cDNA was isolated from human fetal brain RNA by RT-PCR with Thermoscript RT (Invitrogen) and Platinum Taq DNA polymerase (Invitrogen) and cloning either in pCMV-HA or pCMV-myc vectors (CLONTECH Laboratories, Inc.). All constructs were verified by sequencing.

293T, HeLa, and cos-7 cells were grown in Dulbecco's modified Eagle's medium containing 10% fetal calf serum. Cells were transfected using the standard calcium phosphate method (16) or Lipofectamine 2000 reagent (Invitrogen).

Coimmunoprecipitation. 293T cells were cotransfected with the indicated expression plasmids for CYLD and TRIP. Cells were lysed 36 h after transfection in RIPA buffer (50 mM Tris-HCl, pH 7.4, 1% NP-40, 10 mM NaF, 0.25% deoxycholate, 150 mM NaCl, 1 mM EDTA, 1 mM PMSF, and protease inhibitors; Roche). The supernatant after centrifugation was used for immunoprecipitations with anti-FLAG antibody and protein G–sepharose beads. Beads were washed several times in RIPA buffer. Immunoprecipitates were analyzed by immunoblot using FLAG M2 (Sigma-Aldrich), HA (Y-11; Santa Cruz Biotechnology, Inc.), or myc (A-14; Santa Cruz Biotechnology, Inc.) antibodies.

Far Western. TRIP cDNA and fragments thereof were subcloned into the pGEX-4T1 vector (Pharmacia) to generate glutathione *S*-transferase (GST) fusion proteins by induction with 0.1 mM IPTG in BL21 CodonPlus (DE3) RIL bacteria. Equal amounts of protein were separated by SDS-PAGE and transferred to Hybond membranes. After blocking overnight at 4°C in AC buffer (10% glycerol, 100 mM NaCl, 20 mM Tris-HCl, pH 7.6, 0.5 mM EDTA, 0.1% Tween-20, 2% nonfat dry milk), membranes were incubated for 2 h with a RIPA buffer extract from transfected 293T cells diluted in AC buffer. After rinsing the membrane in 20 mM Tris-HCl, pH 7.5, 100 mM NaCl, and 0.1% Tween-20, bound proteins were detected as described above.

Immunofluorescence Microscopy. Cells were grown on coverslips in 6-well plates and transfected as described above. 24–48 h after transfection, cells were fixed in −20°C methanol for 3 min and rehydrated in TBST (0.15 M NaCl, 0.02 M Tris-HCl, pH 7.4, 0.1% Triton X-100). Slides were blocked (TBST, 2% BSA) and incubated with the indicated primary antibodies. Coverslips were then incubated with biotinylated horse anti–mouse IgG, and finally with Alexa Fluor 488 goat anti–rabbit IgG $F(ab')_2$ fragment and streptavidin Texas red. Fluorescence images were collected with a DMIRBE TCSNT laser confocal microscope (Leica). No cross talk between the green and red channel was detected.

NF-κB Reporter Assay. HeLa or 293T cells seeded (8×10^4 cells/well) in 24-well plates were transfected 24 h later with 0.6 μg of the indicated expression plasmids, and 0.2 μg pKB-luc (17) and 0.01 μg pRL-TK (Promega) as reporter plasmids. Human TNF-α (R&D Systems) or human IL-1β (Apotech) were added as indicated. Cell extracts in Passive Lysis Buffer (Promega) were prepared at the indicated time points and luciferase activities were measured with the Dual-Luciferase Reporter Assay System (Promega). Fold induction (mean ± SEM) was calculated as the ratio of relative luciferase activity from treated and nontreated samples.

Results and Discussion

CYLD Interacts with the COOH-terminal Domain of TRIP. To determine the signal transduction pathways in which CYLD participates, we performed a yeast two hybrid screen using full-length CYLD cDNA as bait and an HaCaT cDNA library (CLONTECH Laboratories, Inc.) as

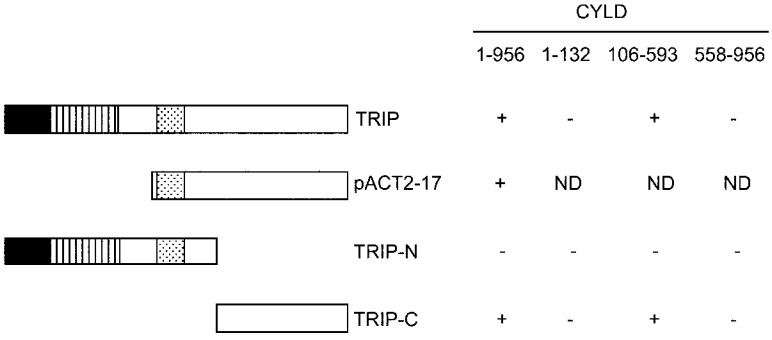

Figure 1. Schematic overview of CYLD–TRIP interactions obtained from yeast two hybrid analysis. The interaction strength between full-length and subdomains of CYLD and TRIP was assessed by measuring α-galactosidase activity in the medium. TRIP-N corresponds to aa 1–289, TRIP-C to aa 290–469, and pACT2–17 to aa 211–469, respectively. The black box denotes the RING domain, the hatched box denotes the coiled coil region, and the punctuate box denotes the leucine zipper domain of TRIP (reference 18).

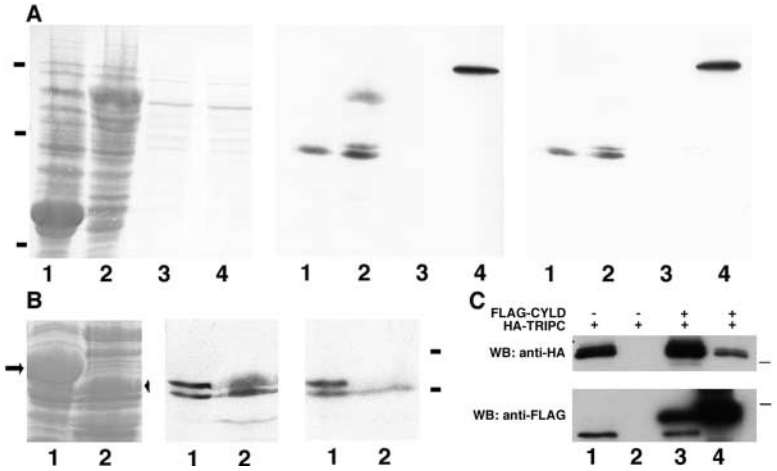

Figure 2. Analysis of the interaction between CYLD and TRIP. (A) Ponceau S staining (left) shows loading of total bacterial extracts expressing GST (lane 1) and GST-TRIP (lane 2), and RIPA extracts from 293T cells either nontransfected (lane 3) or transfected with HA-CYLD (lane 4). Far Western analysis after incubating membrane with extracts from 293T cells transfected with HA-CYLD (middle) or nontransfected (right). Bound proteins were detected with anti-HA antibody. Bars indicate molecular weights of 100, 50, and 20 kD (top to bottom). (B) Ponceau S staining (left) shows loading of total bacterial extracts expressing GST-TRIP-N (lane 1, arrow) and GST-TRIP-C (lane 2, arrowhead). Far Western analysis with extracts from 293T cells transfected either with HA-CYLD (middle) or HA-lacZ (right). Bound proteins were detected with anti-HA antibody. Bars indicate molecular weights of 60 and 40 kD (top to bottom). (C) Coimmunoprecipitation experiments demonstrate interaction of CYLD with TRIP-C in 293T cells. Cells were transfected with equal amounts of FLAG-CYLD and HA-TRIP-C expression vectors. Immunoprecipitates (lanes 2 and 4) obtained with anti-FLAG antibody were analyzed by Western blots with anti-HA (top) and anti-FLAG (bottom) antibodies. Lanes 1 and 3 show input. The bars on the right side mark the molecular weights of 20 (top) and 120 kD (bottom).

prey. Multiple cDNA clones representing different proteins were isolated and characterized by sequencing. One of them, clone pACT2-17, encoded aa 211–469 of TRIP (TRAF-interacting protein; reference 18). The NH_2-terminal half of TRIP contains a RING finger domain, coiled coil region, and a leucine zipper, and interacts with the TRAF domain of TRAF1 and TRAF2 (18).

To map interacting domains of TRIP and CYLD and assess their binding strength we measured α-galactosidase activities. The combination of full-length CYLD with either pACT2-17 or full-length TRIP had similar α-galactosidase activities, indicating that only the COOH-terminal part (aa 211–469) of TRIP is required for interacting with CYLD. To define more precisely the region of TRIP

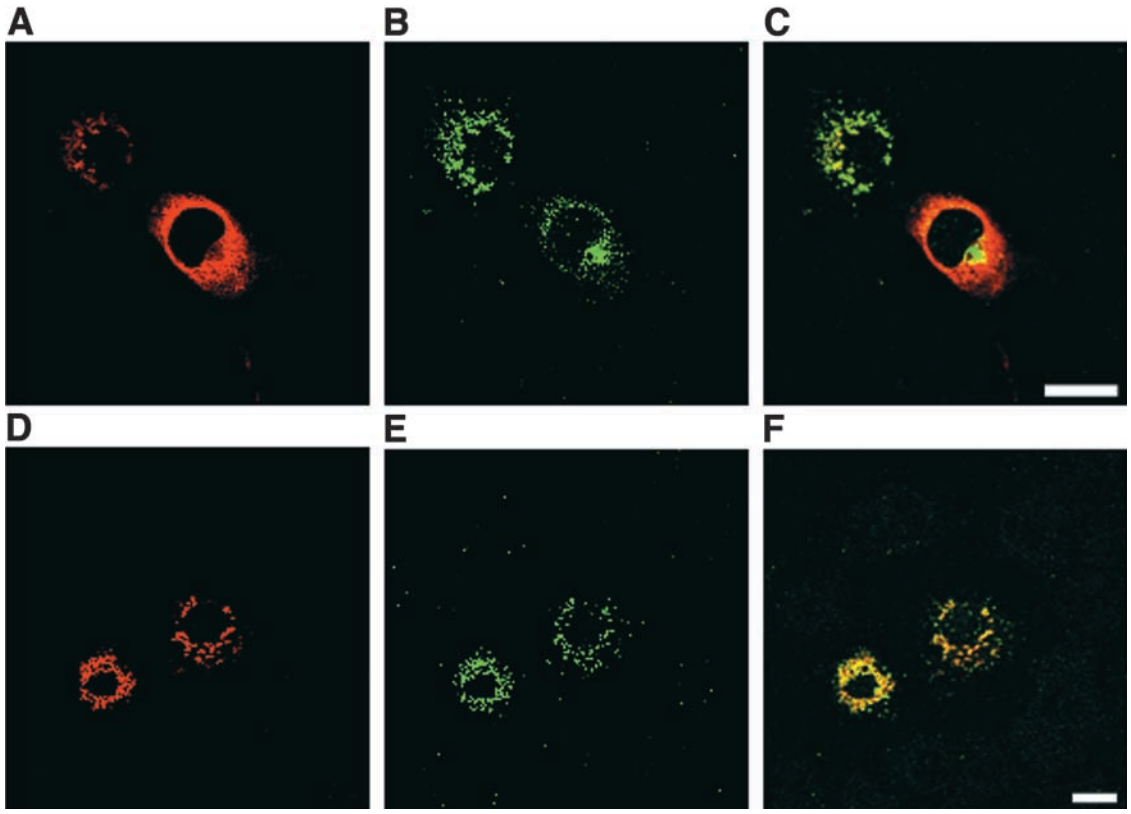

Figure 3. CYLD and TRIP are colocalized in perinuclear compartment of cos-7 cells. Cells were cotransfected with myc-TRIP and FLAG-CYLD and their cellular localization was analyzed by staining with anti-FLAG (red) and anti-myc (green) antibodies and confocal immunofluorescence microscopy. Two examples for CYLD (A and D), TRIP staining (B and E), and the merged pictures (C and F) are shown. Bar, 20 μm. Sections are 0.081 μm.

binding to CYLD, we constructed pGADT7 expression vectors for TRIP-N (aa 1–289) and TRIP-C (aa 290–469). Only TRIP-C interacted positively with full-length CYLD, suggesting that the last 179 aa of TRIP carry the CYLD binding site (Fig. 1). Furthermore, only the central domain (aa 106–593) but neither N-(aa 1–132) nor C-(aa 558–956) terminal domains of CYLD interacted with full-length TRIP. These results were confirmed by analyzing colony formation and blue color of the different combinations of domains on high stringency plates.

To confirm the CYLD–TRIP interaction in mammalian cells we performed Far Western analysis with GST-TRIP fusion proteins and cell extracts of 293T cells transfected with HA-tagged full-length CYLD. Consistent with the findings in yeast, CYLD bound to GST-TRIP (Fig. 2 A) and GST-TRIP-C (Fig. 2 B), but not to GST-TRIP-N or GST. HA-lacZ did not bind to GST-TRIP-C (Fig. 2 B), indicating that CYLD binding to TRIP-C is specific. Coimmunoprecipitation experiments with anti-FLAG antibody demonstrated that HA-TRIP-C interacted with FLAG-CYLD, whereas TRIP-C was not precipitated in the absence of FLAG-CYLD (Fig. 2 C). Whether full-length TRIP is immunoprecipitated by CYLD could not be tested because most of the overexpressed TRIP was not soluble in the RIPA buffer used for coimmunoprecipitations. Collectively, these experiments established the interaction of the central domain of CYLD with the COOH-terminal portion of TRIP (Fig. 1).

CYLD and TRIP Colocalize in the Perinuclear Compartment. Confocal immunofluorescence analysis of cos-7 cells overexpressing FLAG-CYLD and myc-TRIP showed good colocalization of the two proteins in the perinuclear region (Fig. 3). An identical staining pattern was observed in cos-7 cells expressing either CYLD or TRIP, suggesting that CYLD–TRIP interaction does not change their subcellular localizations.

CYLD Inhibits TNF-α–mediated NF-κB Activation. The identification of TRIP, which down-regulates TNF-α–induced NF-κB activity (18), as CYLD interactor, prompted us to study the effect of CYLD on NF-κB activation. NF-κB reporter assays in HeLa cells transiently transfected with pCruzCYLD1 or pHATRIP showed that CYLD inhibited in a dose-dependent manner TNF-α–mediated activation of the NF-κB reporter gene similar to TRIP (Fig. 4 A). In contrast, transfection of COOH-terminal truncated CYLD mutants TT14 (aa 1–481) and TT19 (aa 1–558; reference 9), as well as the mutant del153–536, where most of the central portion of CYLD was deleted, showed no effect on TNF-α up-regulation of NF-κB activity (Fig. 4 B). This provides evidence that both the deubiquitinating activity and the central domain, which interacts with TRIP, are required for CYLD repression of NF-κB activation.

Recently, it has been reported that CYLD inhibits the activation of NF-κB by IL-1β in 293T cells (19). However, earlier reports indicated that TRIP does not regulate the activation of NF-κB by IL-1β in 293 cells (18). Experiments to reinvestigate whether TRIP affected the IL-1β activation of NF-κB clearly showed that TRIP repressed NF-κB activation in 293T and HeLa cells (Fig. 4 C and unpublished data). We conclude that CYLD and TRIP probably cooperate in the regulation of the IL-1β pathway in some but not all cell lines. Because CYLD is not interacting with TRAF6 (19), it will be interesting to explore whether TRIP interacts with TRAF6.

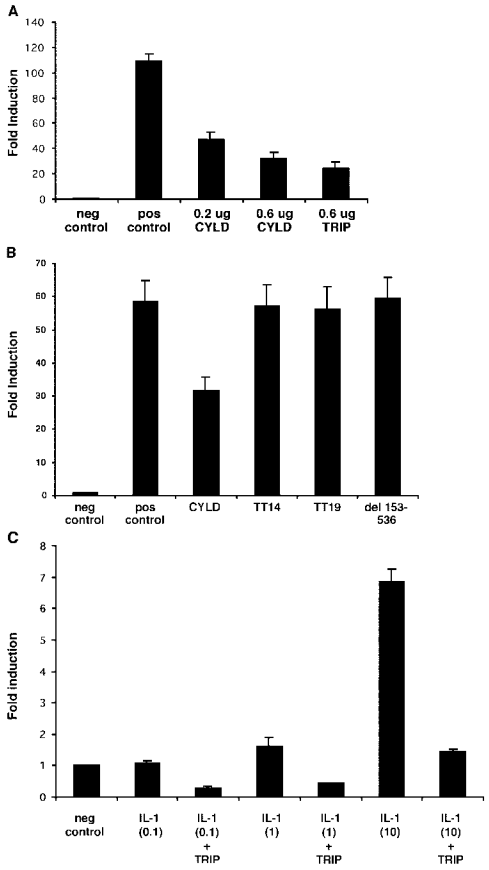

Figure 4. CYLD and TRIP inhibit cytokine-mediated activation of NF-κB. HeLa (A and B) or 293T (C) cells were treated with 10 ng/ml TNF-α for 20 h or IL-1β for 6 h (at concentrations indicated in ng/ml). (A) Dose-dependent effect of CYLD on NF-κB activation by TNF-α. (B) Effect of CYLD mutants (0.6 μg plasmid) TT14, TT19, and del153-536 on NF-κB activity induced by TNF-α. (C) TRIP (0.6 μg plasmid) inhibits IL-1β activation of NF-κB. The results from one representative experiment from a total of three (A) or two (B and C) experiments are shown. Each data point was performed in triplicate.

Interestingly, CYLD interacts with NEMO (IKKγ; references 19–21) and TRAF2 (19, 21), both of which are recruited to the TNF receptor upon ligand binding. Furthermore, CYLD inhibits NF-κB activation by TNF and TLR/IL-1 family members (19–21). Mechanistically, CYLD removes lysine-63–linked ubiquitin chains from TRAF2, TRAF6, and NEMO, whereas lysine-48–linked ubiquitin chains are not degraded by CYLD (19–21). This deubiquitinating activity is required for CYLD inhibition of NF-κB activation (19–21) and is likely affected by mutations found in cylindroma patients. The removal of the

ubiquitin moieties by CYLD presumably prevents the assembly of a multiprotein complex activating IKK and subsequently NF-κB.

The COOH-terminal domain of TRIP interacts with CYLD, whereas the NH_2-terminal region binds to TRAF2 (18). This argues for the presence of a ternary complex of CYLD, TRIP, and TRAF2, which would block NF-κB activation by sequestering TRAF2 away from the TNF receptor. Physiologically there might be a finely tuned balance between TRIP and TRAF2 levels deciding whether there is an excess of TRAF2 and activation of NF-κB or an excess of TRIP and no activation. Although it has not been formally shown that TRIP is ubiquitinated and degraded by the proteasome upon receptor activation, the RING domain of TRAF2 could ubiquitinate TRIP. CYLD could stabilize TRIP by removing the ubiquitins and thereby blocking NF-κB activation. This model is supported by reporter assays (Fig. 4 B) demonstrating a requirement for the TRIP-interacting and ubiquitin-specific protease domain of CYLD to down-regulate NF-κB.

How do these findings explain cylindroma formation and the tissue-specific predisposition of this adnexal tumor despite the ubiquitous tissue expression of CYLD? Inactivation of the CYLD gene should result in persistent activation of NF-κB in targeted cells. Although up-regulated NF-κB activity leads to cancer in other tissues (22), the situation in skin is more complex. Sustained NF-κB activity in the basal cell layer decreased cell proliferation (23) and mice where NF-κB activity is permanently inhibited by overexpressing degradation-resistant IκBα develop squamous cell carcinomas (24) or hyperplastic epithelium (23). Furthermore, coexpression of an oncogenic Ras mutant and the mutant IκBα cooperated to form highly invasive squamous cell carcinomas in human epidermal keratinocyte grafts (25). These data imply that inhibition not activation of NF-κB can lead to epidermal proliferation and neoplastic transformation. However, expression of IκBα superrepressor in hair follicles and epidermal appendages and results from transgenic mice expressing β-galactosidase under the control of NF-κB are consistent with a requirement for NF-κB activation in hair follicle and eccrine gland formation (23, 24, 26, 27). The complex epidermal phenotype displayed by IκBα repressor mice is almost identical to those of tabby, downless, and crinkled mice carrying mutations in the genes for EDA, EDAR, and EDARADD, suggesting that NF-κB activity is required for EDA/EDAR signaling in hair follicle and epidermal appendage formation (28). In humans, congenital deficiencies of sweat glands and hair are known in patients suffering from hypo- or anhydrotic ectodermal dysplasia, which are caused by mutations in EDAR or EDA genes (29, 30). CYLD depresses NF-κB activity induced by EDAR and XEDAR (19, 21), suggesting that loss of CYLD function leads to increased NF-κB signaling, cell proliferation, and up-regulation of antiapoptotic factors in apocrine cells of the skin where cylindromas arise (1, 2). Furthermore, TRIP together with CYLD could negatively regulate EDA/EDAR/EDARADD signaling because EDARADD interacts with TRAF1, TRAF2, and TRAF3 (28). Preliminary data from RT-PCR demonstrated that TRIP is expressed in scalp skin, human foreskin, and epidermis.

In summary, we have identified TRIP as interactor of CYLD and show that CYLD inhibits NF-κB activation by TNF-α. The implication of the interacting pair CYLD–TRIP in NF-κB signaling adds more players to the already highly complex regulation of NF-κB activity influencing proliferation and differentiation of epidermis and skin appendages.

We are indebted to Caroline Lehmann and Ahmed Al-Jaibaji for expert technical assistance. We thank Drs. Tschopp and Schneider for helpful discussions.

This work was supported by a Swiss National Science Foundation grant (31-064015.00) to M. Huber, by Swiss Cancer League grants (1150-09-2001) to M. Huber and (00758-11-1998) to D. Hohl, a RATP grant to D. Hohl, and a grant from the Swedish Cancer Fund to R. Toftgård.

Submitted: 16 July 2003
Accepted: 17 October 2003

References

1. Lever, W., and G. Schaumburg-Lever. 1990. Histopathology of the Skin. 7th ed. Lippincott, JB, Philadelphia. 848 pp.
2. Tellechea, O., J. Reis, O. Ilheu, and A. Poiares Baptista. 1995. Dermal cylindroma. *Am. J. Dermatopathol.* 17:260–265.
3. Burrows, N., R. Russell Jones, and N. Smith. 1992. The clinicopathological features of familial cylindromas and trichoepitheliomas (Brooke-Spiegler syndrome): a report of two families. *Clin. Exp. Dermatol.* 17:332–336.
4. Biggs, P.J., R. Wooster, D. Ford, P. Chapman, J. Mangion, Y. Quirk, D.F. Easton, J. Burn, and M.R. Stratton. 1995. Familial cylindromatosis (turban tumour syndrome) gene localised to chromosome 16q12-q13: evidence for its role as a tumour suppressor gene. *Nat. Genet.* 11:441–443.
5. Biggs, P.J., P. Chapman, S.R. Lakhani, J. Burn, and M.R. Stratton. 1996. The cylindromatosis gene (cyld1) on chromosome 16q may be the only tumour suppressor gene involved in the development of cylindromas. *Oncogene.* 12:1375–1377.
6. Takahashi, M., E. Rapley, P. Biggs, S. Lakhani, D. Cooke, J. Hansen, E. Blair, B. Hofmann, R. Siebert, G. Turner, et al. 2000. Linkage and LOH studies in 19 cylindromatosis families show no evidence of genetic heterogeneity and refine the CYLD locus on chromosome 16q12-q13. *Hum. Genet.* 106: 58–65.
7. Thomson, S., S. Rasmussen, J. Zhang, and M. Wallace. 1999. A new hereditary cylindromatosis family associated with CYLD1 on chromosome 16. *Hum. Genet.* 105:171–173.
8. Verhoef, S., C.T.R.M. Schrander-Stumpel, V.D. Vuzevski, A. Tempelaars, L.A.J. Jansen, G.A.M. Malfeyt, T.L. Ceelen, D. Lindhout, D.J.J. Halley, and A.M.W. van den Ouweland. 1998. Familial cylindromatosis mimicking tuberous sclerosis complex and confirmation of the cylindromatosis locus, CYLD1, in a large family. *J. Med. Genet.* 35:841–845.
9. Bignell, G., W. Warren, S. Seal, M. Takahashi, E. Rapley, R. Barfoot, H. Green, C. Brown, P. Biggs, S. Lakhani, et al.

2000. Identification of the familial cylindromatosis tumour-suppressor gene. *Nat. Genet.* 25:160–165.
10. Leonard, N., R. Chaggar, C. Jones, M. Takahashi, A. Nikitopoulou, and S.R. Lakhani. 2001. Loss of heterozygosity at cylindromatosis gene locus, CYLD, in sporadic skin adnexal tumours. *J. Clin. Pathol.* 54:689–692.
11. Riehemann, K., and C. Sorg. 1993. Sequence homologies between four cytoskeleton-associated proteins. *Trends Biochem. Sci.* 18:82–83.
12. D'Andrea, A., and D. Pellman. 1998. Deubiquitinating enzymes: a new class of biological regulators. *Crit. Rev. Biochem. Mol. Biol.* 33:337–352.
13. Wilkinson, K.D. 1997. Regulation of ubiquitin-dependent processes by deubiquitinating enzymes. *FASEB J.* 11:1245–1256.
14. Borodovsky, A., H. Ovaa, N. Kolli, T. Gan-Erdene, K.D. Wilkinson, H.L. Ploegh, and B.M. Kessler. 2002. Chemistry-based functional proteomics reveals novel members of the deubiquitinating enzyme family. *Chem. Biol.* 9:1149–1159.
15. Kaufman, R.J., M.V. Davies, V.K. Pathak, and J.W.B. Hershey. 1989. The phosphorylation state of eucaryotic initiation factor 2 alters translational efficiency of specific mRNAs. *Mol. Biol. Cell.* 9:946–958.
16. van der Eb, A.J., and F.L. Graham. 1980. Assay of transforming activity of tumor virus DNA. *Methods Enzymol.* 65:826–839.
17. Roger, T., J. David, M.P. Glauser, and T. Calandra. 2001. MIF regulates innate immune responses through modulation of Toll-like receptor 4. *Nature.* 414:920–924.
18. Lee, S.Y., S.Y. Lee, and Y. Choi. 1997. TRAF-interacting protein (TRIP): a novel component of the tumor necrosis factor receptor (TNFR)– and CD30–TRAF signaling complexes that inhibits TRAF2-mediated NF-κB activation. *J. Exp. Med.* 185:1275–1285.
19. Kovalenko, A., C. Chable-Bessia, G. Cantarella, A. Israel, D. Wallach, and G. Courtois. 2003. The tumour suppressor CYLD negatively regulates NF-κB signalling by deubiquitination. *Nature.* 424:801–805.
20. Brummelkamp, T.R., S.M.B. Nijman, A.M.G. Dirac, and R. Bernards. 2003. Loss of the cylindromatosis tumour suppressor inhibits apoptosis by activating NF-κB. *Nature.* 424:797–801.
21. Trompouki, E., E. Hatzivassilliou, T. Tsichritzis, H. Farmer, A. Ashworth, and G. Mosialos. 2003. CYLD is a deubiquitinating enzyme that negatively regulates NF-κB activation by TNFR family members. *Nature.* 424:793–796.
22. Karin, M., Y. Cao, F.R. Greten, and Z.-W. Li. 2002. NF-κB in cancer: from innocent bystander to major culprit. *Nat. Rev. Cancer.* 2:301–310.
23. Seitz, C.S., Q. Lin, H. Deng, and P.A. Khavari. 1998. Alterations in NF-κB function in transgenic epithelial tissue demonstrate a growth inhibitory role for NF-κB. *Proc. Natl. Acad. Sci. USA.* 95:2307–2312.
24. van Hogerlinden, M., B. Lundh Rozell, L. Aehrlund-Richter, and R. Toftgard. 1999. Squamous cell carcinoma and increased apoptosis in skin with inhibited Rel/nuclear factor-κB signaling. *Cancer Res.* 59:3299–3303.
25. Dajee, M., M. Lazarov, J.Y. Zhang, T. Cai, C.L. Green, A.J. Russell, M.P. Marinkovich, S. Tao, Q. Lin, Y. Kubo, et al. 2003. NF-κB blockade and oncogenic Ras trigger invasive human epidermal neoplasia. *Nature.* 421:639–643.
26. Schmidt-Ullrich, R., S. Memet, A. Lilienbaum, J. Feuillard, M. Raphael, and A. Israel. 1996. NF-κB activity in transgenic mice: developmental regulation and tissue specificity. *Development.* 122:2117–2128.
27. Schmidt-Ullrich, R., T. Aebischer, J. Hülsken, W. Birchmeier, U. Klemm, and C. Scheidereit. 2001. Requirement of NF-κB/Rel for the development of hair follicles and other epidermal appendices. *Development.* 128:3843–3853.
28. Headon, D.J., S.A. Emmal, B.M. Ferguson, A.S. Tucker, M.J. Justice, P.T. Sharpe, J. Zonana, and P.A. Overbeek. 2001. Gene defect in ectodermal dysplasia implicates a death domain adaptor in development. *Nature.* 414:913–916.
29. Headon, D.J., and P.A. Overbeek. 1999. Involvement of a novel TNF receptor homologue in hair follicle induction. *Nat. Genet.* 22:370–374.
30. Monreal, A.W., B.M. Ferguson, D.J. Headon, S.L. Street, P.A. Overbeek, and J. Zonana. 1999. Mutations in the human homologue of mouse dl cause autosomal recessive and dominant hypohidrotic ectodermal dysplasia. *Nat. Genet.* 22: 366–369.